Atmos. Meas. Tech. Discuss., 4, 7405–7434, 2011
www.atmos-meas-tech-discuss.net/4/7405/2011/
doi:10.5194/amtd-4-7405-2011

Atmospheric Measurement Techniques Discussions

The mathematical principles and design of the NAIS – a spectrometer for the measurement of cluster ion and nanometer aerosol size distributions

S. Mirme and A. Mirme

Institute of Physics, University of Tartu, Ülikooli 18, 50090 Tartu, Estonia

Received: 30 May 2011 – Accepted: 30 October 2011 – Published: 13 December 2011

Correspondence to: S. Mirme (sander.mirme@ut.ee)

Published by Copernicus Publications on behalf of the European Geosciences Union.

Abstract

The paper describes the Nanometer aerosol and Air Ion Spectrometer (NAIS) – a multi-channel aerosol instrument capable of measuring the distribution of ions (charged particles and cluster ions) of both polarities in the electric mobility range from 3.2 to 0.0013 $cm^2\,V^{-1}\,s^{-1}$ and the distribution of aerosol particles in the size range from 2.0 to 40 nm. We introduce the principles of design, data processing and spectrum deconvolution of the instrument.

1 Introduction

Formation of aerosol by nucleation of particles and their subsequent growth have been observed in the atmosphere almost everywhere around the world (Kulmala et al., 2004). The formed particles, initially of nanometer size, may grow further, participate in cloud formation and influence the radiation balance and ultimately the climate. On local scales, these particles may be deleterious to atmospheric visibility and to human health.

Despite the growing interest, the driving factors of the phenomenon are still poorly studied (Kulmala et al., 2007b). One reason for this is the difficulty of measuring aerosol particles in the size range of a few nanometers under atmospheric conditions.

A number of aerosol instruments can sense fine nanometer range particles and measure their concentration in the atmosphere using the principle of condensational growth and optical counting, but information about particle sizes variations is practically lost. Some information about particle size can be acquired by combining the readings of several counters with different cut-off sizes (Kulmala et al., 2007a) or by analyzing the pulse height of the instrument response (Marti et al., 1996). These methods exhibit some dependence on particle chemical composition.

The particle distribution in a broad particle size range is measured by spectrometers that use electrical mobility classification (e.g. SMPS, FMPS). The smallest mobility

AMTD
4, 7405–7434, 2011

equivalent particle size that can be measured by these instruments is typically 3 nm. It is often limited by the condensation particle counter (CPC) used for particle detection (Vanhanen et al., 2011; Lehtipalo et al., 2009).

Distributions of particles with sizes below 3 nm can be measured by some instruments that sense air ions (particles with an electric charge), e.g. the AIS (Mirme et al., 2007), BSMA (Tammet, 2006). As these instruments do not sense uncharged particles, a big fraction of aerosol is left unmeasured.

2 The principle

An electrical aerosol instrument assesses the total concentration of particles (including the uncharged fraction) based on a known probability distribution of electric charge on a particle after the aerosol has been charged in well-defined conditions. The particles are detected electrically by their carried electric charge. Thus, the limitation of the CPC principle is avoided. Also, the method is not sensitive to the chemical composition of particles. Only large purely dielectric non-conductive particles ($d > 500$ nm) are detected incorrectly, because they obtain less electric charge, but those are unlikely to occur in normal atmosphere.

A common way to charge particles is to pass the aerosol through an aerosol neutralizer right before the measurement unit. The obtained charge is strongly dependent on particle size. For smaller particles the charging probability decreases and particle loss increases, which causes the electric response signal to gradually drop. Thus, the the lower limit of the measurable particle size range is primarily determined by measurement uncertainties.

Here we introduce the Nanometer aerosol and Air Ion Spectrometer (NAIS, developed by Airel Ltd., Estonia) that uses the principle of electrical aerosol spectrometry. The NAIS has been specifically designed for monitoring of atmospheric nanometer aerosol. It can operate for long periods in a wide range of ambient conditions, from polluted downtown to remote forest, to measure the size distributions of naturally-charged

AMTD
4, 7405–7434, 2011

particles (ions) of both polarities as well as uncharged particles. It is based on the Air Ion Spectrometer (AIS, Mirme et al., 2007).

Like the AIS, the NAIS consists of two multichannel electrical mobility analyzer columns operating in parallel. The columns differ by the polarity of the ions measured, but are otherwise identical (Fig. 1). The aerosol is contemporarly mobility-classified in the mobility analyzers and measured with an array of 21 electrometers per column.

Both columns have a software controlled sample preconditioning unit in front of the analyzers, which allows the instrument to switch between either detecting naturally-charged particles (ions) or all particles (including the uncharged fraction) by using unipolar charging. The mobility range in ions mode is from 3.2 to 0.0013 $cm^2\,V^{-1}\,s^{-1}$. This covers both the cluster ions ranging (at 20 °C) from 3.2 to 0.5 $cm^2\,V^{-1}\,s^{-1}$ and the aerosol ions ranging from 0.4 to 0.0013 $cm^2\,V^{-1}\,s^{-1}$ (Hõrrak et al., 2000). The size range in particles mode is from below 2 nm up to 40 nm given in Stokes-Millikan mobility equivalent diameter at NTP conditions.

The two similar measurement columns with opposite polarity operating in parallel allow the NAIS to detect variations of natural electric charge balance in the atmosphere and possible effects of electric charge polarity on charging of nanometer-size aerosol.

3 Methods

There are more than ten NAIS instruments in use today. The technology has been developed gradually and implemented into new instruments along the way. The first five instruments built were very similar to the AIS, only with added particle charging. We describe the second generation NAIS, which has an updated airflow system and much enhanced data acquisition, but most of the information is valid for the older instruments as well.

AMTD
4, 7405–7434, 2011

3.1 Sample preconditioning

The sample preconditioning unit consists of a discharger, an electric filter, a charger and another electric filter (called the post-filter). The charger and post-filter correspond to the electrical measurement principle (Flagan, 1998), where the instrument consists of aerosol charging followed by mobility analysis and data acquisition.

In ions mode, all components of the preconditioning unit are switched off, so the aerosol sample is left unmodified and only naturally-charged particles are sensed by the electric mobility analyzer. In this case the NAIS operates just like the AIS.

In particles mode, the main charger is switched on and the instrument detects all particles. The post-filter is used to remove traces of charger ions. In this operating mode, the NAIS is similar to the Electrical Aerosol Spectrometer (EAS, Tammet et al., 2002). To improve the instrument performance when measuring aerosol with non-steady state charge distribution, the discharger may be switched on (alternative charging mode). This provides some neutralization of the aerosol sample and so reduces the effect of the particle initial charge on the measurement result.

When only the discharger and the adjacent filter are switched on, then no detectable particles can enter the analyzer. This is called the offset mode and it is used to periodically verify the instrument operation (e.g. evaluate noise levels and measure parasitic currents).

3.2 Charging

To assess the aerosol particle size distribution, it is necessary to know the charge distribution of particles exiting the charger as a function of charging conditions and particle size.

The NAIS uses unipolar corona chargers – essentially a corona needle on the axis of a cylindrical volume (Fig. 2). The ions from the tip of the needle travel across the aerosol sample flow and attach to particles mainly by thermal diffusion. The

AMTD
4, 7405–7434, 2011

charging ion concentration is maintained at a constant level by stabilizing the current that reaches the electrode surrounding the charging space.

The process of a particle acquiring electric charge is viewed as a flux of ions onto the particle. The flux is calculated using the kinetic theory (Podolsky, 1977) inside the limiting sphere around a particle (Fuchs, 1963). The radius of the limiting sphere is a parameter specified at the calibration.

The probability distribution of electric charge on particles after passing the charger is calculated by integrating a birth-death differential equation (Boisdron and Brock, 1970) considering the charger characteristics. An integral formula (Salm, 1992) is used to produce the complete distribution. The formula allows calculation of the charger output charge distribution for an arbitrary initial charge distribution (e.g. a bipolar equilibrium charging state). A typical result for the NAIS charger is presented in Fig. 3.

The charger is characterized with the charging parameter α (Tammet, 1992):

$$\alpha = \frac{1}{\varepsilon_0} \int \sigma \, \mathrm{d}t, \tag{1}$$

where ε_0 is the vacuum permittivity and $\sigma = ez_i n$ is the electrical conductivity of air (e is the elementary charge, z_i is the electrical mobility of charging ions, and n the ion concentration). The exact value of the charging parameter is determined at the calibration.

The design of the discharger is similar to that of the subsequent main charger but it works in the opposite electrical polarity. In offset mode, when only the discharger is switched on, particles are charged to the wrong polarity for the respective analyzer, so the measured signal only consists of the parasitic (offset) currents and measurement noise. By knowing the offset signal, measurement uncertainties can be significantly decreased and reliability of the results improved.

When the instrument operates in the particles measurement mode, the enabling of the discharger in addition to the main charger can provide neutralization of particles as initially charged particles are effectively discharged with opposite polarity charger ions either in the discharger or main charger, depending on their initial charge.

AMTD
4, 7405–7434, 2011

3.3 Mobility analysis

The measurement process that follows the preconditioning is again similar to that of AIS. The only addition is that, in particles measurement mode, the probability distribution of electric charge on particles must be taken into account for calculating the size distribution.

The mobility analyzer consists of a number of cylindrical electrodes (Fig. 4). The central electrode is divided into several sections, each biased at a different fixed electric potential. The charge collecting outer electrodes are connected to electrometric amplifiers at near ground potential, which in turn are connected to a data acquisition system. The charged aerosol is sucked into a circular slit near the central electrode. The clean sheath air is introduced near the outer electrode. The particles travel along the analyzer, and those with the same charge electrical polarity as the central electrode are pushed towards the outer electrodes by a radial electric field. The particles that have been deposited on a collecting section pass their charge on to the respective amplifier.

The mobility analysis follows the generic aspiration theory (Tammet, 1970). According the theory, the movement of a charged particle (z) in an analyzer is determined by the air flow rate (Φ) and the electric field ($C \cdot U$ product) that is crossed by the particle while traveling inside the analyzer:

$$z = \frac{\Phi \cdot \varepsilon_0}{C \cdot U}. \quad (2)$$

The formula determines the relationship between three parameters: air flow rate, mobility and analyzer capacitance. Fixing one of them fixes the ratio of the other two. So an ion with the mobility z attaching to an outer electrode has passed the flow rate Φ and the electric field CU. This allows calculation of the attachment locations of ions with different mobilities entering the analyzer at different flow rates. The formula can be modified for the analyzer, consisting of multiple sections as follows:

AMTD
4, 7405–7434, 2011

$$z_n = \frac{(\Phi_a + \Phi_s) \cdot \varepsilon_0}{\sum_{i=0}^{n} C_i \cdot U_i}, \quad (3)$$

where Φ_a is the sample aerosol flow rate, Φ_s is the sheath flow rate, and z_n is the lowest (limiting) mobility of particles reaching the the section n.

The capacitances between the collecting sections and sections of central electrodes for the NAIS are presented in Table 1. The table also shows the voltages of the respective sections. Note that the collecting sections are not matched with the central sections: collecting sections 9, 13 and 17 have some capacitance with two adjacent central sections. This is used to cover a wide mobility range quite smoothly with a limited number of central sections. The calculated theoretical responses (transfer functions) for each section of the mobility analyzer are quite broad (Fig. 5) and have a varying mobility resolution.

3.4 Relationship between particle size and electrical mobility

Once particles are charged, their electrical mobility distribution can be measured with a mobility analyzer. In order to proceed from that to particle size distribution, the particle mobility must be related to the particle size and electric charge.

The conversions by Millikan (Fuchs, 1964) and by Tammet (Tammet, 1995) have been considered. NAIS uses the well-known Millikan formula, keeping in mind that the Tammet correction can be introduced later:

$$z_{\text{Millikan}} = e \frac{1 + \frac{\lambda}{r}\left[a + b \exp\left(-c \frac{r}{\lambda}\right)\right]}{6 \pi \eta r} \quad (4)$$

where a, b and c are empirical constants, e is the elementary charge, λ is the particle mean free path, and η is the viscosity of air. The mobility of a particle of a given size is a function of ambient atmospheric pressure and temperature.

AMTD
4, 7405–7434, 2011

Newer generation NAIS instruments automatically adjust their sample and sheath airflow speeds so that the particle sizing and volume sample flow remain constant regardless of air pressure.

Under NTP conditions, the NAIS uses the sheath flow value $\Phi_s = 1000\,\mathrm{cm}^3\,\mathrm{s}^{-1}$ and the sample flow value $\Phi_a = 500\,\mathrm{cm}^3\,\mathrm{s}^{-1}$. If we consider Eq. (2), the size of the classified particle remains invariant of air pressure if Φ_s and Φ_a are chosen so that the expression $\frac{\Phi_s+\Phi_a}{z}$ remains invariant of air pressure.

In case of small particles, for which the mean free path is much larger than particle radius, Eq. (4) can be simplified (Tammet, 1995). After substituting λ and η, we get the Eq. (5):

$$\lim_{r\to 0} z_{\mathrm{Millikan}} = \frac{e\,(a\,+\,b)}{6\,\pi\,r^2}\,\frac{1.256}{P}\,\sqrt{\frac{k\,T}{m_g}} \propto \frac{\sqrt{T}}{P} \tag{5}$$

where m_g is the mass of air molecule, P is air pressure and T is temperature.

In NAIS, the sample flow rate Φ_a is kept constant. Considering Eqs. (2) and (5), this means that the size classification remains air pressure invariant if Φ_s is chosen, so that the following relation holds:

$$\left(\Phi_s' + \Phi_a'\right)\frac{\sqrt{T'}}{P'} = \left(\Phi_s + \Phi_a'\right)\frac{\sqrt{T}}{P}, \tag{6}$$

where Φ_s', Φ_a', T' and P' are the corresponding variables under standard conditions. This allows the instrument to be used in varying conditions, e.g. for airborne measurements (Mirme et al., 2010).

3.5 Mathematical model

The instrument response of the NAIS is a set of electric currents that are generated by the flux of ions precipitating to the analyzer sections. Each section current y_i equals

AMTD
4, 7405–7434, 2011

the sum of the charge flux of all aerosol particles of the size distribution $f(r)$ that reach the section i:

$$y_i = \int \left[e \sum_q q\, G(i, z)\, P(q, r) \right] f(r)\, \mathrm{d}r, \quad (i = 1, \ldots, n), \tag{7}$$

where $G(i, z)$ is the response of analyzer section i to unit concentration of singly charged ions with mobility z, and $P(q, r)$ is the probability that a particle with radius r carries q elementary charges (e).

In the case of an ion analyzer (electric charge $q = 1$ and charging probability function $P = 1$), the response function G is equal to the amount of airflow from which the ions of the given mobility are attached to the given analyzer section. In case of a particle analyzer, the charging probability $P(q, r) < 1$ (Fig. 3) and size equivalent mobility $z = z(q, r)$ functions are in effect.

The response function $G(i, z)$ for NAIS is presented in Fig. 5. The channels up to 12 are located quite densely on the mobility scale to provide higher mobility resolution in the cluster ion range (negative cluster ions $z \simeq 1.7\,\mathrm{cm^2\,V^{-1}\,s^{-1}}$, positive $z \simeq 1.3\,\mathrm{cm^2\,V^{-1}\,s^{-1}}$).

Despite the different peak values of different channels, the sum of the responses at any mobility is close to $\Phi_a = 500\,\mathrm{cm^3\,s^{-1}}$. Some decrease at higher mobilities is caused by particle loss at the inlet. The loss factor is arbitrary and is found during the calibration.

The system of Eq. (7) links the unknown aerosol distribution $f(r)$ with the measured currents y_i ($i = 1, \ldots, n$). The equations should fully consider the instrument specificity (charging, mobility analysis, etc.).

3.6 Electric current measurement

The electric currents collected on the outer electrodes are very small: in the range of 1–3 fA per electrode in the cluster ion range and even smaller in intermediate ion range (Hõrrak, 2001).

AMTD
4, 7405–7434, 2011

The NAIS uses integrating electrometric amplifiers where the fluxes of electric charge are collected on high quality electrical capacitors. The output voltages of the amplifiers are proportional to the collected electric charge and the change of the voltage is proportional to incoming charge, i.e. to the aerosol current.

The integrating measurement principle allows for the best possible signal to noise ratio for electric current measurements. It is also well suited for the NAIS as the signal is collected continuously almost without any breaks – no signal is missed regardless of measurement frequency.

The NAIS uses a high measurement rate (10 to 15 times per electrometer per second). Several signal prosessing steps are used before reducing the signal to typically 10 s to 2 min average records (Fig. 6).

Firstly, the electric current values are corrected for the offset currents measured periodically during the offset operating mode.

Often short spikes occur in the electric current signal. These are probably caused by the random decay of radioactive particles deposited on the electrodes. The frequency of spikes depends on how much debris has collected on the electrodes. An outlier detection algorithm is used to discard the false signal measurements.

The excessively high measurement rate enables employment of optimal signal processing (ARMA filter). The electric current signal is passed through a matched digital filter to flatten the noise frequency distribution (noise whitening). This improves the effectiveness of averaging in case of short periods, i.e. 1 to 10 s.

The collected charge on the capacitors needs to be cleared every once in a while. In a NAIS, the electrometers will automatically reset when the output signal reaches the upper or lower limit of the integrator. Signal from that electrometer is ignored for the duration of the reset and the settling, which takes about ten seconds. At low concentrations, resets can happen about once a day for each electrometer, which practically does not affect the measurements.

AMTD
4, 7405–7434, 2011

4 Spectrum model

The task of spectrometry is to solve instrument response Eq. (7), i.e. to find the aerosol distribution $f(r)$ from the measured channel currents.

The task is mathematically incorrect. An approximate solution is possible if we limit the information required for the description of the aerosol distribution. Therefore, we estimate the aerosol distribution as a sum of m elementary distributions of predefined shapes $\phi^j(r)$ (Fig. 7):

$$f(r) = \sum_j \phi_j \cdot \phi^j(r), \quad (j = 1, \ldots, m). \tag{8}$$

The set is chosen based on the capabilities of the instrument and the data inversion. This way, an aerosol distribution is described by a set of coefficients ϕ_j (a spectrum) and the integral instrument response equations (Eq. 7) can be transformed into a set of linear equations (Eq. 9) or the equivalent matrix form (Eq. 10):

$$y_i = \sum_j \mathbf{H}_{ij} \cdot \phi_j, \quad (i = 1, \ldots, n) \tag{9}$$

$$\boldsymbol{y} = \mathbf{H} \cdot \boldsymbol{\phi}. \tag{10}$$

The instrument record vector $\boldsymbol{y}$ consists of section currents y_i and the spectrum vector $\boldsymbol{\phi}$ consists of coefficients ϕ_j. Matrix $\mathbf{H}$ can be called an apparatus matrix. The matrix element $\mathbf{H}_{ij}$ is the response of the analyzer section i to the elementary aerosol distribution $\phi^j(r)$ (Eq. 11).

$$\mathbf{H}_{ij} = \int \left[e \sum_q q\, G(i, z(q, r))\, P(q, r) \right] \phi^j(r)\, \mathrm{d}r \tag{11}$$

AMTD
4, 7405–7434, 2011

4.1 Evaluation of the spectrum

For the NAIS, the distribution is found by solving the apparatus equation (Eq. 10) in respect to spectrum $\boldsymbol{\phi}$. The inversion is performed with the Gauss-Markov method of least squares:

$$\boldsymbol{\phi} = \left(\mathbf{H}^T \mathbf{D}^{-1} \mathbf{H}\right)^{-1} \mathbf{H}^T \mathbf{D}^{-1} \boldsymbol{y}. \quad (12)$$

The measurement uncertainties are described by a covariance matrix **D**, with the elements $D_{ii} = \Delta y_i^2$ being the variances of section currents. The uncertainty of the spectrum is then given by Eq. (13):

$$\mathbf{W} = \left(\mathbf{H}^T \mathbf{D}^{-1} \mathbf{H}\right)^{-1}. \quad (13)$$

The ordinary distribution can be estimated from spectrum $\boldsymbol{\phi}$ with Eq. (8). Commonly, the distribution estimate is presented as a piecewise linear number density function.

4.2 Regularization of the inversion

In the case of the NAIS, the number of elementary spectra is larger than the number of electometers. This means that the information matrix (Eq. 14) is always ill posed and it is not possible to invert it directly:

$$\mathbf{V} = \mathbf{H}^T \mathbf{D}^{-1} \mathbf{H}. \quad (14)$$

This is solved by using Tikhonov regularization (Tikhonov, 1963). The method allows increasing the rank of the matrix and thus correcting the ill-posedness (Lemmetty et al., 2005). The diagonal elements of **V** are amplified:

$$\mathbf{V}'_{ij} = \begin{cases} \mathbf{V}_{ij} & \text{if } i \neq j, \\ \mathbf{V}_{ij} \cdot (1 + \lambda_i) & \text{if } i = j \end{cases}, \quad (15)$$

where $\boldsymbol{\lambda}$ is an arbitrary regularization vector.

AMTD
4, 7405–7434, 2011

A quasi-optimal regularization is reached by performing a two-pass inversion. Initially, to make the inversion possible at all, the regularization parameter is set to a small constant: $\lambda_i = 0.001$.

The second inversion is performed using a regularization vector based on uncertainty levels obtained from the first pass. The regularization vector $\boldsymbol{\lambda}$ is calculated as the ratio of error $\mathbf{W}' = \mathbf{V}'^{-1}$ to spectrum $\boldsymbol{\phi}$:

$$\lambda'_i = K \cdot \frac{\mathbf{W}'_{ii}}{\phi_i^2} \tag{16}$$

where K is a constant in the range 0.1 to 1. The values of $\boldsymbol{\lambda}$ and K are not critical and are chosen during the calibration of an instrument.

4.3 Correction of negative concentration values

The inversion does not impose any constraints on the spectrum $\boldsymbol{\phi}$ and so negative values can appear in the solutions for measurements at low concentrations. A simple procedure is used to remove these.

If negative values appear, the inversion is repeated with the assumption that the previously most negative element of $\boldsymbol{\phi}$ is virtually zero and the corresponding column in the instrument matrix is dropped. Usually, two or three iterations are sufficient to remove all negative elements.

The procedure may increase the total concentration estimate. However, due to the nature of the inversion and significant overlapping of the elementary distributions, any correction of a spectrum element is balanced by changes in neighboring elements and the estimated spectrum still fits the measured currents. As a result, the effect remains below the level of measurement uncertainties.

AMTD
4, 7405–7434, 2011

5 Calibration methods

The goal of the calibration is to find the best values for the instrument matrix elements $\mathbf{H}_{ij}$ (Eq. 11). General methods for the calibration of multi-channel aerosol size spectrometers (Mirme, 1987; Tammet and Noppel, 1992) can be used for this. In principle, each one of the parallel channels in each of the different operating modes of the instrument requires calibration.

The calibration of NAIS is based on a mathematical model of the instrument, which is used to calculate the channel currents (Eq. 7) for the set of elementary spectra. Most of the model parameters can be measured directly. The rest are found by fitting the model to experimental calibration results.

The analyzer transfer function $G(i, z)$ (Eq. 7) is derived in a straightforward way and it is verified by calibration measurements in ions mode where the charging probability member is equal to one.

In the aerosol mode, additionally the charger and post-filter are activated and need to be taken into account: both $G(i, z)$ and $P(q, r)$ are in effect. $G(i, z)$ is already verified by the ions mode calibrations as the analyzer operates identically in all modes. Only the aerosol charging probability function $P(q, r)$ has to be calibrated.

However, particle charging is both theoretically and technically poorly defined. So a preliminary calibration is made on a theoretical basis with some estimated probable values. The parameters are fine tuned during the calibration procedure when the measurement data is verified against well-defined laboratory aerosols (Mirme, 1987; Tammet and Noppel, 1992).

Consequently, the NAIS uses a mixed calibration: the model parameters that can be measured with high accuracy are fixed and only verified later during calibration. These parameters include the analyzer geometry, electrode voltage (Table 1), air flow rates and electrometer sensitivity. From this, an approximate calibration is built, which is used to experimentally assess the remaining, poorly defined parameters, such as the particle loss factor of the inlet tract.

AMTD
4, 7405–7434, 2011

6 Results and discussion

In this paper we describe the second generation NAIS, which was developed with the primary motivation to enable the instrument to operate at varying altitudes on board an aircraft, but also to improve the reliability of regular measurements. The most important enhancements over the first generation are a new data acquisition system and an updated airflow scheme; the older instruments lack the automatic airflow adjustment, automatic charger/filter tuning and the signal processing steps that rely on a high measurement rate.

The calibration and verification of NAIS is a complex task. All the instruments have been briefly tested and calibrated at the facilities of University of Tartu (Mirme et al., 2007). Their performance has been more thoroughly studied in several calibration and intercomparison experiments at the University of Helsinki.

In 2008, five NAIS and five AIS instruments were compared and calibrated at the University of Helsinki using high resolution and HAUKE type DMA-s for mobility references, and a CPC and a aerosol electrometer for concentration references (Asmi et al., 2009). The NAIS-s overestimated the size of negative ions by 20–52 % and the size of positive ions by 24–54 %. The concentration measurements from NAIS were shown to be reliable at medium and high concentrations, but at lower concentrations the NAIS-s showed some background noise.

In 2010, six NAIS and five AIS instruments were evaluated at the University of Helsinki regarding particle size/mobility and concentration using mobility standards and silver particles covering the size range between 1 and 40 nm (Gagné et al., 2011). The instruments were compared to a differential mobility particle sizer (DMPS), a BSMA (Tammet, 2006) and an Ion-DMPS. The experiments showed that the mobility detection of the AIS and NAIS instruments is reliable, provided that the instrument is clean and the flows are not obstructed. That said, the NAIS can overestimate the concentration by a factor of 2–3 in the particles measurement mode.

AMTD
4, 7405–7434, 2011

Nevertheless, the results should be regarded as quite good considering that the design goal of the AIS/NAIS was to provide researchers of atmospheric aerosol phenomena the most comprehensive information on the nucleation and aerosol formation processes, including electrical effects. In these studies, it is important that the instrument can reliably track the variations of the distributions and that it requires little maintenance. It should also be considered that features of specific comparison setups have a strong effect on comparison results: this includes the sample aerosol preparation, its electrical state, verification, and transport to the instrument.

Due to the different measurement modes and particle/ion size/mobility range, already the proper preparation of verification aerosol is a challenging task. For example, almost all well-defined aerosols are produced using aerosol classifiers. That suits well for the NAIS if ion mode is verified. However, that is not very representative for particle mode because atmospheric aerosol is normally close to a steady state charge distribution. An additional neutralizer corrects the aerosol but also adds a lot of ions generated by the neutralizer itself. These ions are detected and confuse the first measurement channels and thus need to be removed before entering the instrument.

Another feature of NAIS compared to scanning-type instruments is the great number of parallel channels. This ensures a fast and correct response to any variation of aerosol, but has the drawback that a deviation of the geometry of a specific channel not accounted for in calibration may produce a deviation in output distribution. However, that is outweighed by the reliability, low maintenance and undisturbed reaction in any varying environment.

There are more than ten NAIS instruments in use today. The spectrometers have been measuring around the world in many different urban and rural environments, as well as on board an aircraft and a hot air balloon (see Hirsikko et al., 2011 for references).

A number of NAIS and AIS instruments were used in the EUCAARI (European Integrated Project on Aerosol Cloud Climate Air Quality Interactions; Kulmala et al., 2009; Manninen et al., 2010; Kerminen et al., 2010) project measurement stations in 2008

AMTD
4, 7405–7434, 2011

and 2009. During the EUCAARI LONGREX airborne measurement campaign, the NAIS for the first time measured neutral sub-3 nm particles in the free troposphere at altitutdes up to 8 km (Mirme et al., 2010).

7 Conclusions

In this article we have presented the principles of operation of an aerosol instrument – Nanometer aerosol and Air Ion Spectrometer (NAIS) – that can measure the distributions of ions in both polarities as well as uncharged particles. Ions are detected in the electric mobility range from 3.2 to 0.0013 $cm^2\,V^{-1}\,s^{-1}$ and aerosol particles are detected in the size range from 2.0 to 40 nm. The instrument measures the whole size range of both polarities of ions simultaneously, which allows achieving high time resolution. Alternatively, the instrument measures uncharged particles in the whole size range by using both positive and negative particle charging (Fig. 8).

The NAIS has proven to be an invaluable instrument in studying atmospheric new particle formation.

Acknowledgements. This research has been in part supported by European Commission 6th Framework program projects: EUCAARI, contract no. 036833-2 (EUCAARI), by the Estonian Science Foundation through grants 8342 and 8417, and the Estonian Research Council Targeted Financing Project SF0180043s08.

AMTD
4, 7405–7434, 2011

References

Asmi, E., Sipilä, M., Manninen, H. E., Vanhanen, J., Lehtipalo, K., Gagné, S., Neitola, K., Mirme, A., Mirme, S., Tamm, E., Uin, J., Komsaare, K., Attoui, M., and Kulmala, M.: Results of the first air ion spectrometer calibration and intercomparison workshop, Atmos. Chem. Phys., 9, 141–154, doi:10.5194/acp-9-141-2009, 2009. 7420

Boisdron, T. and Brock, J. R.: On the stochastic nature of the acquisition of elecric charge and radioactivity by aerosol particles, Atmos. Environ., 4, 35–50, 1970. 7410

Flagan, R. C.: History of Electrical Aerosol Measurements, Aerosol Sci. Tech., 28, 301–380, 1998. 7409

Fuchs, N. A.: On the stationary charge distribution on aerosol particles in bipolar ionic atomosphere, Geofis. Pura Appl., 56, 185–193, 1963. 7410

Fuchs, N. A.: The Mechanics of Aerosols, Pergamon Press, Oxford, 1964. 7412

Gagné, S., Lehtipalo, K., Manninen, H. E., Nieminen, T., Schobesberger, S., Franchin, A., Yli-Juuti, T., Boulon, J., Sonntag, A., Mirme, S., Mirme, A., Hõrrak, U., Petäjä, T., Asmi, E., and Kulmala, M.: Intercomparison of air ion spectrometers: an evaluation of results in varying conditions, Atmos. Meas. Tech., 4, 805–822, doi:10.5194/amt-4-805-2011, 2011. 7420

Hirsikko, A., Nieminen, T., Gagné, S., Lehtipalo, K., Manninen, H. E., Ehn, M., Hõrrak, U., Kerminen, V.-M., Laakso, L., McMurry, P. H., Mirme, A., Mirme, S., Petäjä, T., Tammet, H., Vakkari, V., Vana, M., and Kulmala, M.: Atmospheric ions and nucleation: a review of observations, Atmos. Chem. Phys., 11, 767–798, doi:10.5194/acp-11-767-2011, 2011. 7421

Hõrrak, U.: Air ion mobility spectrum at a rural area, Ph.D. thesis, University of Tartu, 2001. 7414

Hõrrak, U., Salm, J., and Ammet, H.: Statistical characterization of air ion mobility spectra at Tahkuse Observatory: Classification of air ions, J. Geophys. Res.-Atmos., 105, 9291–9302, 2000. 7408

Kerminen, V.-M., Petäjä, T., Manninen, H. E., Paasonen, P., Nieminen, T., Sipilä, M., Junninen, H., Ehn, M., Gagné, S., Laakso, L., Riipinen, I., Vehkamäki, H., Kurten, T., Ortega, I. K., Dal Maso, M., Brus, D., Hyvärinen, A., Lihavainen, H., Leppä, J., Lehtinen, K. E. J., Mirme, A., Mirme, S., Hõrrak, U., Berndt, T., Stratmann, F., Birmili, W., Wiedensohler, A., Metzger, A., Dommen, J., Baltensperger, U., Kiendler-Scharr, A., Mentel, T. F., Wildt, J., Winkler, P. M., Wagner, P. E., Petzold, A., Minikin, A., Plass-Dülmer, C., Pöschl, U., Laaksonen, A., and Kulmala, M.: Atmospheric nucleation: highlights of the EUCAARI project and future

AMTD
4, 7405–7434, 2011

directions, Atmos. Chem. Phys., 10, 10829–10848, doi:10.5194/acp-10-10829-2010, 2010. 7421
Kulmala, M., Vehkimäki, H., Petäjä, T., Maso, M., Lauri, A., Kerminen, V.-M., Birmili, W., and McMurry, P. H.: Formation and growth rates of ultrafine atmospheric particles: A review of observations, J. Aerosol Sci., 35, 143–176, 2004. 7406
Kulmala, M., Mordas, G., Petäjä, T., Grönholm, T., Aalto, P., Vehkamäki, H., Gaman, A., Herrmann, E., Sipilä, M., Riipinen, I., Manninen, H., Hämeri, K., Stratmann, F., Birmili, W., and Wagner, P. E.: The Condensation Particle Counter Battery (CPCB): A New Tool to Investigate the Activation Properties of Nanoparticles, J. Aerosol Sci., 38, 289–304, 2007a. 7406
Kulmala, M., Riipinen, I., Sipilä, M., Manninen, H. E., Petäjä, T., Junninen, H., Maso, M. D., Mordas, G., Mirme, A., Vana, M., Hirsikko, A., Laakso, L., Harrison, R. M., Hanson, I., Leung, C., Lehtinen, K. E., and Kerminen, V.-M.: Towards direct measurement of atmospheric nucleation, Science, 318, 89–92, 2007b. 7406
Kulmala, M., Asmi, A., Lappalainen, H. K., Carslaw, K. S., Pöschl, U., Baltensperger, U., Hov, Ø., Brenquier, J.-L., Pandis, S. N., Facchini, M. C., Hansson, H.-C., Wiedensohler, A., and O'Dowd, C. D.: Introduction: European Integrated Project on Aerosol Cloud Climate and Air Quality interactions (EUCAARI) – integrating aerosol research from nano to global scales, Atmos. Chem. Phys., 9, 2825–2841, doi:10.5194/acp-9-2825-2009, 2009. 7421
Lehtipalo, K., Sipilä, M., Riipinen, I., Nieminen, T., and Kulmala, M.: Analysis of atmospheric neutral and charged molecular clusters in boreal forest using pulse-height CPC, Atmos. Chem. Phys., 9, 4177–4184, doi:10.5194/acp-9-4177-2009, 2009. 7407
Lemmetty, M., Marjamäki, M., and Keskinen, J.: The ELPI response and data reduction II: Properties of kernel and data inversion, Aerosol Sci. Tech., 39, 583–595, 2005. 7417
Manninen, H. E., Nieminen, T., Asmi, E., Gagné, S., Häkkinen, S., Lehtipalo, K., Aalto, P., Vana, M., Mirme, A., Mirme, S., Hõrrak, U., Plass-Dülmer, C., Stange, G., Kiss, G., Hoffer, A., Töro, N., Moerman, M., Henzing, B., de Leeuw, G., Brinkenberg, M., Kouvarakis, G. N., Bougiatioti, A., Mihalopoulos, N., O'Dowd, C., Ceburnis, D., Arneth, A., Svenningsson, B., Swietlicki, E., Tarozzi, L., Decesari, S., Facchini, M. C., Birmili, W., Sonntag, A., Wiedensohler, A., Boulon, J., Sellegri, K., Laj, P., Gysel, M., Bukowiecki, N., Weingartner, E., Wehrle, G., Laaksonen, A., Hamed, A., Joutsensaari, J., Petäjä, T., Kerminen, V.-M., and Kulmala, M.: EUCAARI ion spectrometer measurements at 12 European sites – analysis of new particle formation events, Atmos. Chem. Phys., 10, 7907–7927, doi:10.5194/acp-10-7907-2010, 2010. 7421
Marti, J. J., Weber, R. J., Saros, M. T., Vasiliou, J. G., and McMurry, P. H.: Modification of the

AMTD
4, 7405–7434, 2011

TSI 3025 condensation particle counter for pulse height analysis, Aerosol Sci. Tech., 25-2, 214–218, 1996. 7406
Mirme, A.: About the calibration of the electrical aerosol spectrometer, Acta et comm. Univ. Tartuensis, 755, 71–79, 1987. 7419
Mirme, A., Tamm, E., Mordas, G., Vana, M., Uin, J., Mirme, S., Bernotas, T., Laakso, L., Hirsikko, A., and Kulmala, M.: A wide range multi-channel Air Ion Spectrometer, Boreal Environ. Res., 12, 247–264, 2007. 7407, 7408, 7420
Mirme, S., Mirme, A., Minikin, A., Petzold, A., Hõrrak, U., Kerminen, V.-M., and Kulmala, M.: Atmospheric sub-3 nm particles at high altitudes, Atmos. Chem. Phys., 10, 437–451, doi:10.5194/acp-10-437-2010, 2010. 7413, 7422
Podolsky, A.: On the computation of the time of capturing ions by aerosol particle, In acta et commentationes Universitatis Tartuensis, 443, 62–73, 1977. 7410
Salm, J.: Unipolar Charging of Initially Charged Aerosol, Acta et comm. Univ. Tartuensis, 947, 68–71, 1992. 7410
Tammet, H.: The aspiration method for the Determination of Atmospheric-Ion Spectra, The Israel Program for Scientific Translations Jerusalem, National Science Foundation, Washington, DC, 1970. 7411
Tammet, H.: On the techniques of aerosol electrical granulometry, Acta et comm. Univ. Tartuensis, 947, 94–115, 1992. 7410
Tammet, H.: Size and mobility of nanometer particles, clusters and ions, J. Aerosol Sci., 26, 459–475, 1995. 7412, 7413
Tammet, H.: Continuous scanning of the mobility and size distribution of charged clusters and nanometer particles in atmospheric air and the Balanced Scanning Mobility Analyzer BSMA, Atmos. Res., 82, 523–535, 2006. 7407, 7420
Tammet, H. and Noppel, M.: Principles of the graduation of an electric aerosol granulometer, Acta et comm. Univ. Tartuensis, 947, 116–124, 1992. 7419
Tammet, H., Mirme, A., and Tamm, E.: Electrical aerosol spectrometer of Tartu University, Atmos. Res., 62, 315–324, 2002. 7409
Tikhonov, A. N.: Solution of incorrectly formulated problem and the regularization method, Soviet Math. Dokl., 4, 1035–1038, 1963. 7417
Vanhanen, J., Mikkilä, J., Lehtipalo, K., Sipilä, M., Manninen, H., Siivola, E., Petäjä, T., and Kulmala, M.: Particle Size Magnifier for nano-CN detection, Aerosol Sci. Tech., 45, 533–542, 2011. 7407

AMTD
4, 7405–7434, 2011

Table 1. The electrical capacitance (in pF) between collecting sections and the four central sections of the NAIS mobility analyzer.

Collecting section	Central section (U_A)			
	9 V	25 V	220 V	800 V
0	3030	0	0	0
1	2531	0	0	0
2	2433	0	0	0
3	2504	0	0	0
4	2913	0	0	0
5	3860	0	0	0
6	5597	0	0	0
7	8250	0	0	0
8	8716	0	0	0
9	4006	4526	0	0
10	0	8693	0	0
11	0	8741	0	0
12	0	9850	0	0
13	0	5850	5235	0
14	0	0	10 656	0
15	0	0	11 149	0
16	0	0	13 558	0
17	0	0	11 784	8061
18	0	0	0	19 053
19	0	0	0	25 330
20	0	0	0	25 472
21	0	0	0	25 510

AMTD
4, 7405–7434, 2011

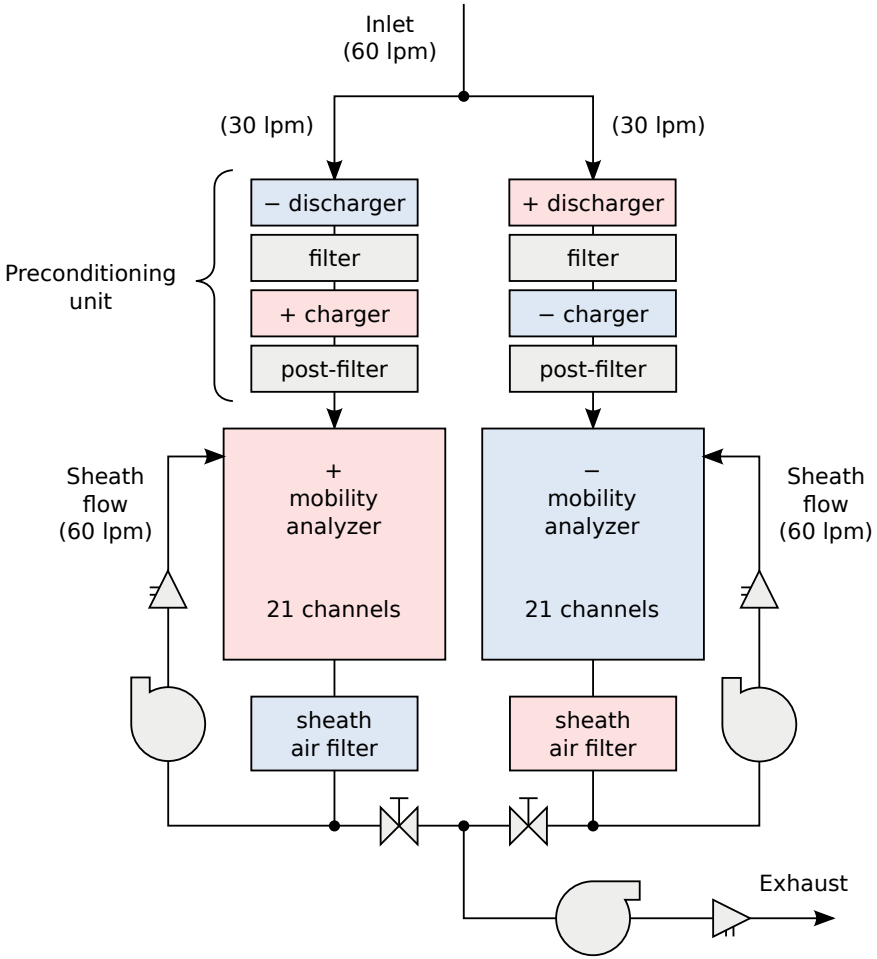

Fig. 1. NAIS measurement flow process.

AMTD
4, 7405–7434, 2011

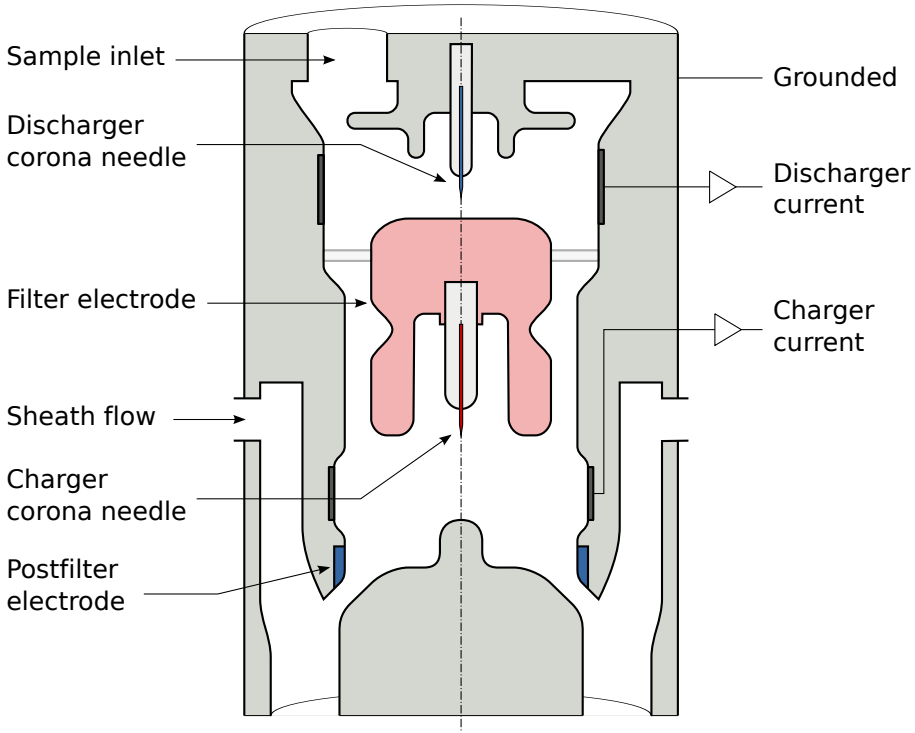

Fig. 2. Schematic of NAIS charger.

AMTD
4, 7405–7434, 2011

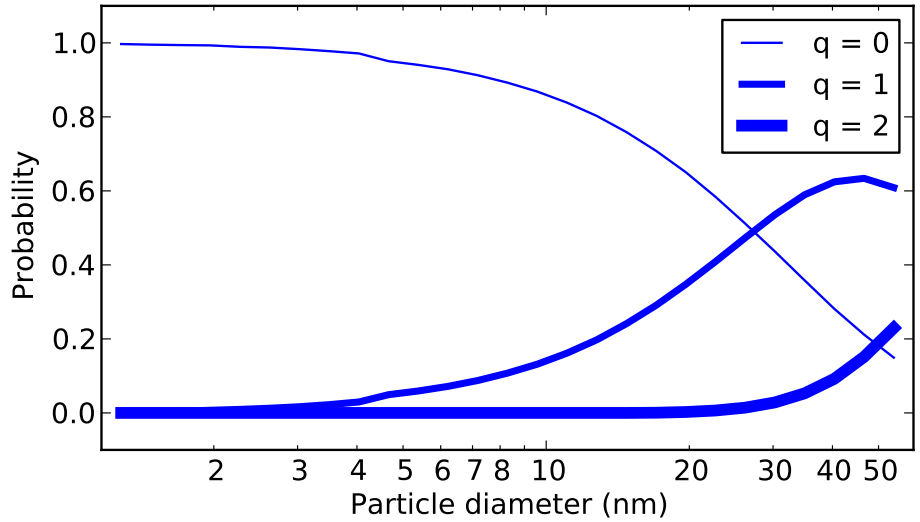

Fig. 3. The probability of parcicles having 0, 1 or 2 elementary charges after passing the main charger of the NAIS.

AMTD
4, 7405–7434, 2011

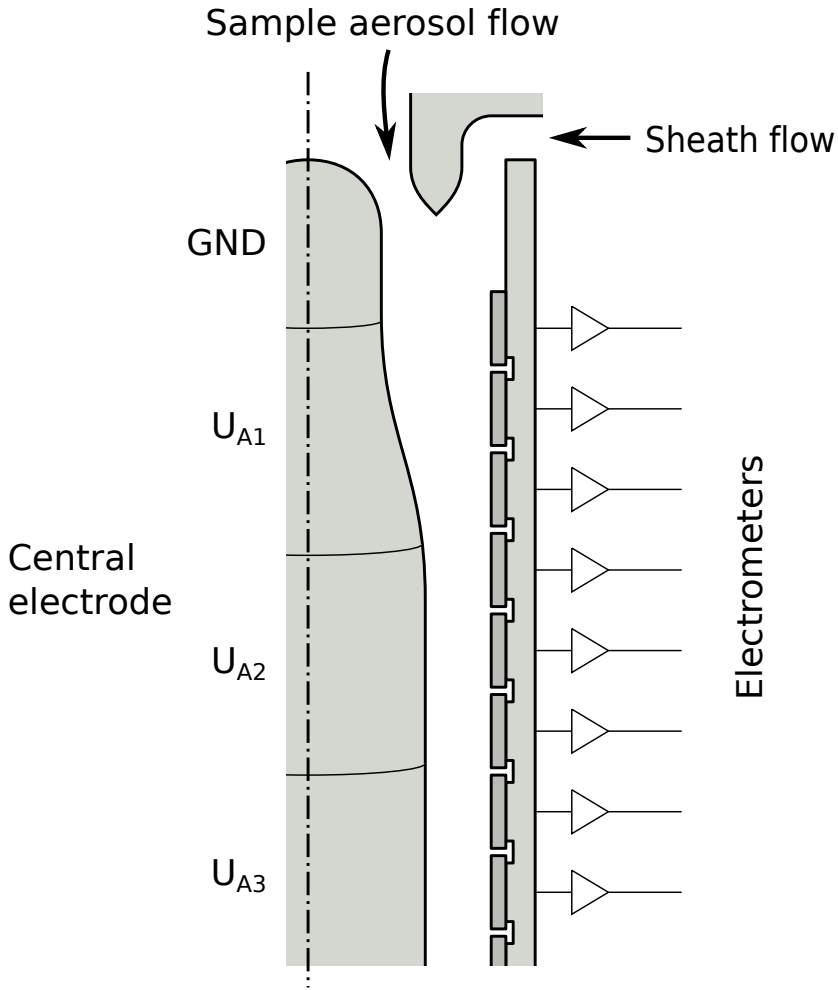

Fig. 4. Schematic of NAIS mobility analyzer.

AMTD
4, 7405–7434, 2011

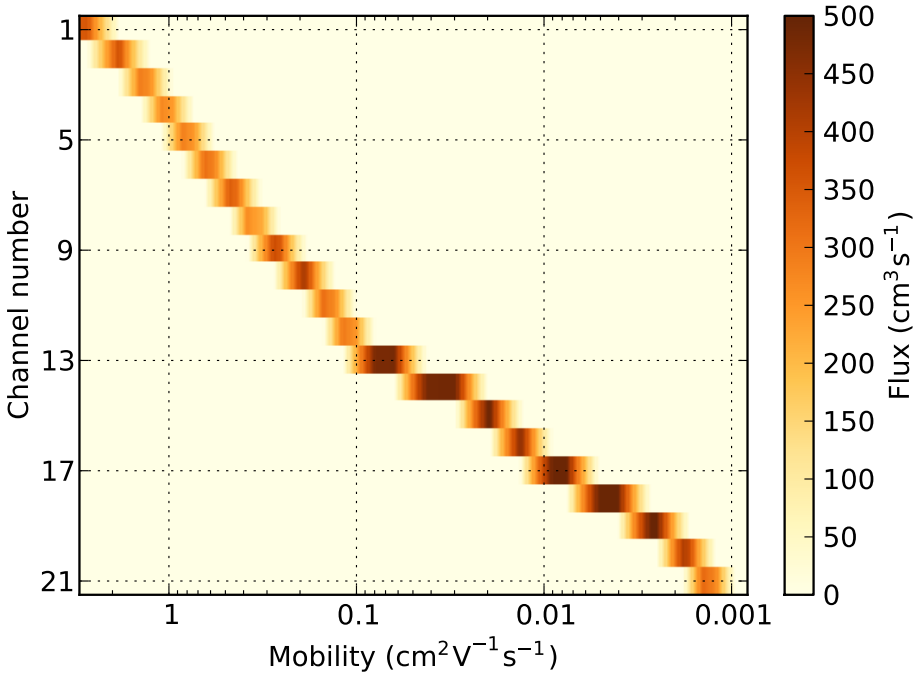

Fig. 5. Analyzer response $G(i, z)$ for the NAIS. It can be seen that the responses for individual channels are overlapping.

AMTD
4, 7405–7434, 2011

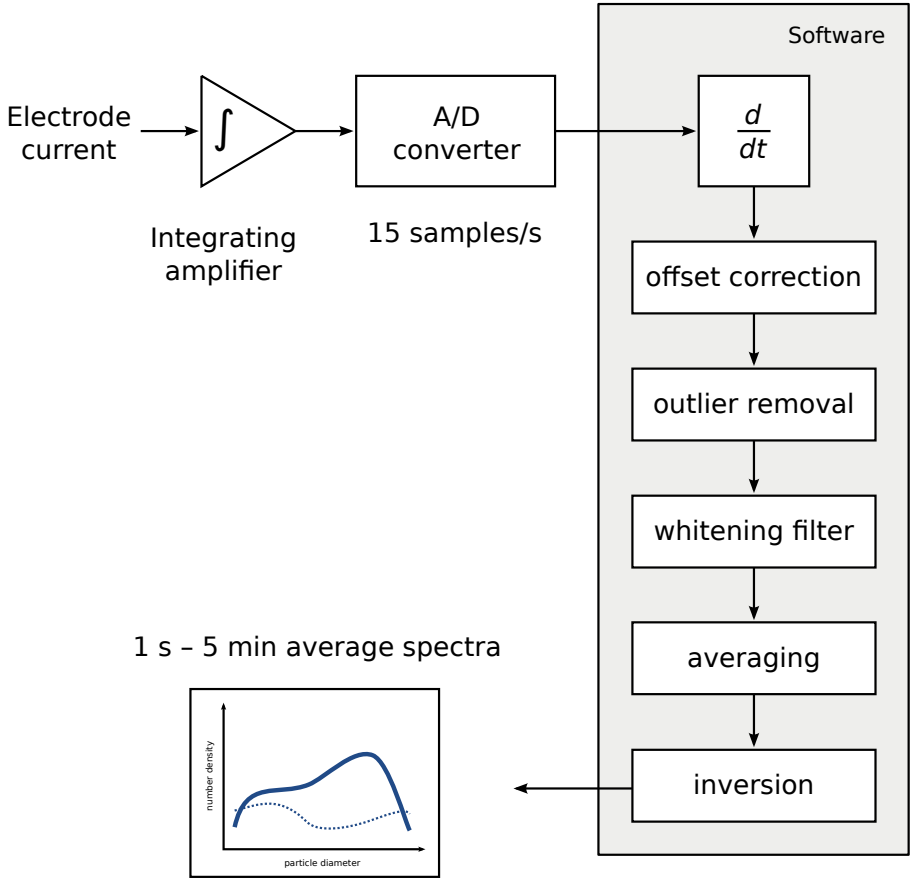

Fig. 6. Signal and data-processing flow diagram of the NAIS.

AMTD
4, 7405–7434, 2011

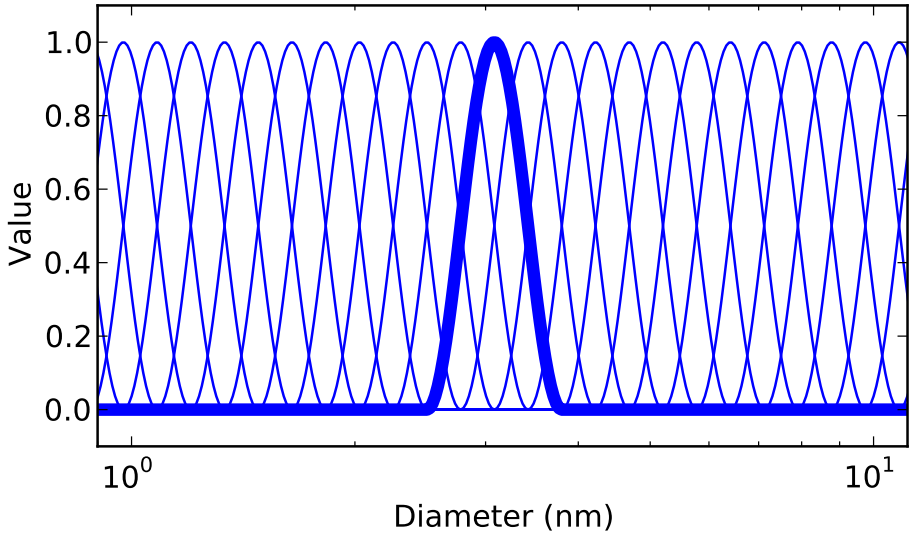

Fig. 7. Part of a typical set of elementary distributions used for NAIS with one distribution highlighted. Commonly the use $\cos^2 x$ in the range $[-\frac{\pi}{2}, \frac{\pi}{2}]$ as the shape for the functions.

AMTD
4, 7405–7434, 2011

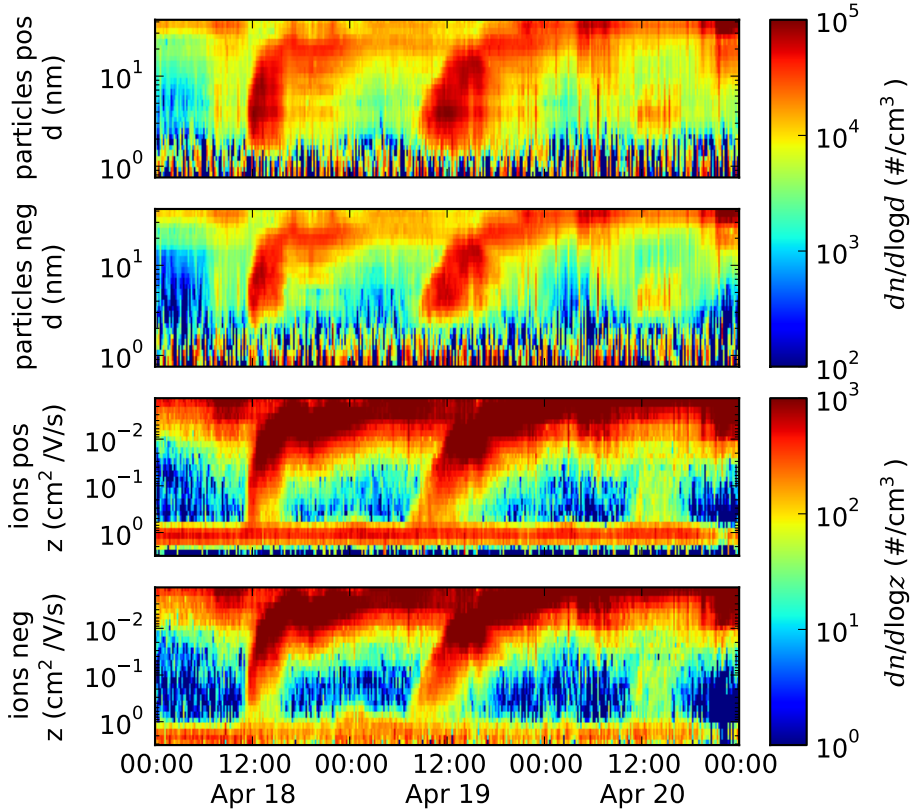

Fig. 8. Typical new particle formation events measured using the NAIS near the town center of Tartu, Estonia.

AMTD
4, 7405–7434, 2011